

Seasonal Change in Titan's Cloud Activity Observed with IRTF/SpeX

E.L. Schaller^{1,2}, M.E. Brown¹, H.G. Roe³

`schaller@ifahawaii.edu`

ABSTRACT

We obtained a 0.8-2.4 micron whole-disk spectrum of Titan on 138 nights between February 2006 and January 2008 with SpeX at the NASA Infrared Telescope Facility. These spectra allow us to probe Titan's surface and troposphere at 6 distinct low opacity window regions in the near infrared. We observe a seasonal difference in the frequency and brightness of Titan's tropospheric clouds during this season (3.5-1.5 Earth years pre vernal equinox) compared with previous seasons Titan has been observed (autumnal equinox and northern winter solstice). These data allow us to constrain the total cloud coverage of Titan's disk on 87% nights to be less than 0.15%. On the 13% of nights on which cloud activity was detected, it covered less than 0.4% of Titan's disk at altitudes of ~ 30 km and did not preferentially occur at any particular Titan longitude. In addition to providing insight into the long and short-term tropospheric cloud evolution on Titan, these data allow us to independently constrain the amount of the surface flux that penetrates at a given wavelength from 0.8-2.4 microns.

Subject headings: Planets and Satellites: Titan – Infrared: Solar System

1. Introduction

Titan provides us with a unique laboratory in which to study a hydrological cycle on a planet other than Earth with a different condensable species (methane on Titan, water on

¹Division of Geological and Planetary Sciences, California Institute of Technology, Pasadena, CA 91125

²now at: Institute for Astronomy, University of Hawaii, Honolulu, HI 96822

³Lowell Observatory, Flagstaff, AZ 86001

Earth). While the presence of Titan’s methane meteorological cycle is now well established, a fundamental understanding of the dynamics of Titan’s weather including the frequencies, locations, and altitudes of Titan’s tropospheric clouds and how these attributes change over Titan’s 29.7-year-long seasonal cycle remains unknown. Understanding Titan’s hydrological cycle is vital for determining the formation mechanisms of fluvial surface features such as lakes in the north polar regions (Stofan et al. 2007; Lorenz et al. 2008) and channels near the equator (Soderblom et al. 2007) that have been observed by Cassini/Huygens.

Tropospheric clouds were first observed in 1995 via near-infrared whole disk spectroscopy on UKIRT by Griffith et al. (1998). Griffith et al. (1998) found that tropospheric clouds caused Titan to become brighter in methane windows (where photons penetrate to the surface and lower atmosphere) while staying the same brightness in methane absorption bands. Titan’s surface features (such as the large Xanadu feature) also cause brightness variations in these windows but they repeat with phase. By measuring Titan’s brightness on the wings of these methane windows (where Titan is moderately opaque and photons penetrate to Titan’s troposphere), Griffith et al. (1998) were able to detect variable tropospheric clouds. Spectra covering these wavelengths of low, moderate, and high opacity along with radiative transfer modeling were used to determine cloud heights and total percent cloud coverage of Titan’s disk (Griffith et al. 1998, 2000). Tropospheric clouds were detected in nearly all observations, were generally found to cover approximately 0.5% of Titan’s disk, and varied on timescales of days and even hours. In addition, in two observations in September 1995, Titan’s clouds brightened considerably, covering between 5-7% of its disk.

The first direct detection of Titan’s clouds was achieved with the Keck adaptive optics system by Brown et al. (2002) and Roe et al. (2002). From 2001-2004, variable tropospheric clouds were regularly observed near Titan’s south pole in adaptive optics images (Bouchez & Brown 2005; Schaller et al. 2006b). Images taken through the H₂(1-0) filter (2.11-2.14 microns) were found to be particularly useful for detecting Titan’s clouds, as this filter probes one of the wavelength regions where the moderate opacity causes most of the surface features to be invisible but tropospheric clouds to clearly stand out. The tropospheric clouds observed in Keck, Gemini, and Palomar adaptive optics images typically contributed about 0.5-1% of the total brightness of Titan’s disk at 2 microns and were generally found within 20 degrees of the south pole (Brown et al. 2002; Bouchez & Brown 2005). However, for approximately one month in October 2004, they increased in brightness to coverages comparable to the 1995 event witnessed by Griffith et al. (1998) (Schaller et al. 2006a).

In addition to the south polar clouds, Roe et al. (2005a,b) and Griffith et al. (2005) also observed clouds at southern midlatitudes (40 S). The streaky, extended morphologies of these clouds were different from the south polar clouds that generally appeared as point sources.

The fact that these clouds were clustered in longitude as well as latitude, led Roe et al. (2005b) to suggest that they were geographically controlled (either due to volcanic outgassing of methane, orography, or other factors). Griffith et al. (2005), who also observed these midlatitude clouds in Cassini images but did not observe a longitude clustering, suggested that their presence at 40 S was related to the changing general circulation patterns supported by the GCM models of Rannou et al. (2006).

Adaptive optics images taken between 2005 and the present have shown that Titan’s south polar cloud activity has markedly decreased. Though Cassini still occasionally observes small clouds (Roberts et al. 2008), it is now rare ($\sim 10\%$) to observe tropospheric cloud activity from the ground in adaptive optics images. In contrast, between 2001- 2005, cloud activity was observed in 97% of adaptive optics images (Schaller et al. 2006b; Bouchez & Brown 2005). Observations from late 2005 showed a hint of cloud activity moving toward more temperate southern latitudes (Schaller et al. 2006b) as Titan’s season changed from southern solstice (October 2002) and is moving toward vernal equinox (August 2009).

In this paper, we present data from a frequent Titan monitoring program begun at the NASA Infrared Telescope Facility which encompasses two years of observations taken during the Cassini prime mission. These observations allow us to detect tropospheric cloud activity and also reveal fundamental properties of Titan’s atmosphere and surface.

2. Observations

In February 2006 we began our frequent Titan spectral monitoring program with the NASA Infrared Telescope Facility (IRTF). We obtained a near infrared spectrum of Titan with SpeX, the facility visible-near infrared spectrograph (Rayner et al. 2003) on 138 nights from February 2006 to January 2008 (Table 1). Observations were taken in the short cross-dispersed (SXD) mode with a 1.6 arcsecond slit. The total spectral range covered was 0.8 to 2.4 microns in 6 orders with a spectral resolution $R \sim 375$ (Figure 1).

On each night, we observed Titan for a total of three minutes of integration time (3 nod pairs of 30 seconds each) while guiding on Titan with the slit guider camera. The slit was oriented in the N/S direction. We performed similar observations of nearby a G dwarf star (3 nod pairs of 15 seconds). From February 2006 through June 2007 this star was HD 77730 (a G2V) and from October 2007 to January 2008 it was HD 89307 (a G0V). Observations of both stars on several nights allowed us to calibrate the data taken with different stars relative to each other. Titan and the reference star were observed so as to minimize the airmass difference between them (the object with the lower right ascension

was observed first). The median difference in airmass between Titan and the star was 0.04 and on only two occasions did it exceed 0.2 (Oct-03-2006 and June-08-2007). In addition, Titan’s median airmass was 1.07 and only exceeded 2 airmasses on the dates mentioned above (Table 1). Including slewing to Titan and internal calibrations (10 flats and an arc lamp) the total time needed to perform these observations was generally under 20 minutes. Spectral data reduction was performed using standard methods employing the SpeXtool version 3.4 package (Cushing et al. 2004). The six Titan and six star spectra were medianed and the combined Titan spectrum was divided by the combined star spectrum to eliminate telluric features. On clear nights, our 3-minute reduced spectra had a signal-to-noise of approximately 350 per pixel in the 2-2.2 micron region (the wavelength region of particular interest for measuring Titan’s tropospheric clouds).

3. Results

3.1. Lightcurves

The 138 spectra of Titan centered at a variety of Titan longitudes (Figures 2, 3) provide us with a unique a posteriori method for determining the degree to which photons from the surface penetrate at a given wavelength. Titan’s large surface albedo variations with phase provide us with a convenient marker with which to determine the contribution of the surface to Titan’s albedo at a given wavelength. This degree to which photons from the surface are able to penetrate at a given wavelength is related to the methane opacity and vertical distribution of aerosols and can be used to constrain radiative transfer models of Titan’s atmosphere. Since 1993, it has been known that Titan’s surface is brightest at approximately 110W longitude. Cassini and ground-based observers with adaptive optics have shown that this bright region is a continent-sized feature now known as Xanadu. In Figure 2 we show H and K band spectra of Titan taken at different central Titan sub-solar longitudes. Each spectrum was normalized to a known high opacity region of Titan’s spectrum (2.2-2.25 microns) where photons penetrate only to the upper stratosphere. We expect that Titan’s flux at this wavelength range should stay relatively constant during our observation period. Spectra taken on nights with different central longitudes show similar albedos in wavelength regions that penetrate to Titan’s stratosphere but have different albedos in the surface penetrating regions. The albedos in surface penetrating wavelength ranges are correlated in H and K.

Using all 138 nights of data taken with different central longitudes over the course of Titan’s 16-day rotation period, we can construct lightcurves at a variety of wavelengths. Figure 3 shows four Titan K-band lightcurves. The amplitude of the lightcurve is strongest at 2.02 microns where methane opacity is low and photons can penetrate to Titan’s surface.

Increasing in wavelength through the K-band, the amplitude of Titan’s lightcurve decreases as methane opacity increases. Individual deviations from the lightcurve (best observed in Figure 3c) are caused by reflective layers above the surface (clouds) and will be discussed in detail in section 3.2. In order to determine the degree to which photons from the surface penetrated at a given wavelength, we measured the amplitude of the lightcurve in 0.0075 micron wavelength bins from 0.8-2.4 microns (Figure 4). The amplitudes of the resulting lightcurves with wavelength reveal the presence of 6 distinct window regions in the near-infrared at 0.8, 0.95, 1.05, 1.27, 1.6, and 2.0 microns where the surface is visible. The 2 micron window is strongest with a surface lightcurve magnitude of approximately 15%.

3.2. Clouds

We can directly compare the amount of cloud activity in this dataset with that seen in a similar dataset from the 1990’s (Griffith et al. 1998 and 2000). Cloud activity was inferred by Griffith et al. (1998) and (2000) by the presence of variability at 2.13-2.17 microns (which was also correlated with variability at 1.62-1.63 microns) on the wings of the 2.0 and 1.6 micron surface penetrating bands. Small variations at this wavelength range (where photons penetrate to the troposphere) corresponded to cloud activity of 0-0.8% at altitudes of approximately 30 km. When they subtracted a spectrum with extremely low cloud activity from all of the other observations, Griffith et al. (2000) saw variability in their residual spectra from 2.13 to 2.15 microns of approximately 0.002 on a daily basis. This type of variability is easily detectable in our dataset, yet on most nights we did not observe it.

In Figure 5 we show residual spectra (the spectrum from 2006-Feb-23 was subtracted from the same six spectra taken at with different central longitudes) compared with residual spectra from Griffith et al. (2000). The 2006-Feb-23 spectrum was chosen as a cloud-free night to subtract from the others because we have simultaneous Gemini coverage on that night showing that no clouds were present. In contrast to the Griffith et al. (2000) residual spectra, most of our spectra deviate from each other shortward of 2.13 microns indicating a lack of clouds in Titan’s troposphere. The three nights of Griffith et al. (2000) observations shown in Figure 5 correspond to 0.3%, 0.5% and 0.7% cloud coverage of Titan’s disk at 30 km altitude. We can convert the residual flux at 2.13 microns to a total cloud coverage by scaling from the observations of Griffith et al. (2000) and find that on most nights Titan’s total cloud coverage was less than 0.15% of its disk (Figure 6). On only 13% of the nights was cloud activity greater than 0.15% with 2-sigma error bars less than 0.15%. A Kolmogorov-Smirnov test of the central longitudes of the nights with clouds compared with the central longitudes of the nights without clouds reveals that they are not statistically different, indicating that

the clouds we have observed are not clustered in longitude. We find a slight increasing trend of cloud activity with time over the past two years. Clouds were observed on sequential nights on two occasions but generally lasted less than one earth night.

4. Discussion

The 138 nights of Titan IRTF observations span less than 7% of a Titan year, the terrestrial equivalent of February 3–28. Titan vernal equinox (i.e. March 21) will occur in August 2009. Our observations show that cloud activity on Titan has markedly decreased in the pre-vernal equinox era compared with the southern summer solstice era (October 2002) (Brown et al. 2002; Roe et al. 2002; Bouchez & Brown 2005; Schaller et al. 2006b) and the autumnal equinox era (1995) (Griffith et al. 1998, 2000). Unlike the Earth, where total cloud activity integrated over the whole surface only changes by several percent over the course of a year (from 58%-62% with northern hemisphere winter being cloudiest) (Thornes 2002; Svensmark & Friis-Christensen 1997), Titan’s disk integrated cloud activity appears to undergo large-scale variations with season and with time (from essentially 0% to over 8%). The month of “February” on Titan appears to be extremely quiescent with only a small amount (covering less than 0.4% of Titan’s disk at 30 km) of tropospheric cloud activity occurring on less than 13% of the nights. In addition, the few nights with cloud activity did not preferentially occur at a specific central longitude of observation, indicating that they may not be formed by the same mechanism or be related to the midlatitude clouds observed by Roe et al. (2005b).

Though Titan’s cloud activity has been rather quiescent of late, we expect that it will eventually resume. Several groups (Tokano 2005; Rannou et al. 2006; Mitchell et al. 2006) have modeled Titan cloud locations with season using General Circulation Models (GCMs). These models make very different predictions regarding when and where Titan’s clouds will resume. Though they all predict a decrease in cloud activity during the present season, the timing and locations of the resurgence are quite different. Rannou et al. (2006) predict that south polar cloud activity should decrease but also predict that cloud activity should be occurring near and 40 N which has never been observed. Rannou et al. (2006) also predict that clouds should begin forming over the north-pole and should be observed as soon as the north-pole comes into view. Tokano (2005) predicts the locations of superadiabatic zones and finds that these should only occur at the poles near the solstices, therefore predicting practically no cloud activity until 2014. Mitchell et al. (2006) predict that clouds should slowly move toward the equator near equinox (essentially following the area of maximum solar insolation with a slight phase lag) with decreased flux until the winter solstice when

clouds will resume with full force near the north pole. The differences in these models are due to the uncertainties regarding the nature of Titan’s surface (its thermal inertia) and other factors such as methane opacity, and haze and aerosol distributions. Saturn’s eccentric orbit around the sun also means that the insolation received at northern summer on Titan is approximately 10% less than that received at southern summer. This fact may lead to differences in southern and northern summer cloud activity. Indeed, the paucity of lakes seen by Cassini Radar in the south pole (Lunine et al. 2008) compared to the abundance in the north pole may perhaps be related to this insolation effect.

While infrequent observations from large telescopes and Cassini flybys are useful for studying the morphologies of clouds and occasional cloud outbursts, only a long-term near-nightly monitoring project has provided the type of dataset necessary to determine the frequency, duration, and altitudes of Titan’s large clouds and daily cloud systems. Especially in this era of decreased cloud activity, near-nightly monitoring is also crucial for catching short-lived events and can provide context for Cassini flybys. Continued observations of Titan’s clouds over the coming years will be critical for understanding the nature of Titan’s hydrological cycle.

5. Conclusions

We have observed a seasonal change in the frequencies and brightnesses of Titan’s tropospheric clouds. We observed cloud activity on only 13% of nights covering between 0.15% and 0.4% of Titan’s disk at altitudes of ~ 30 km. The frequencies and brightnesses of Titan’s clouds have markedly decreased in the pre-vernal equinox era (2006-2008) compared with the time surrounding summer solstice (2001-2005) and autumnal equinox (1995-1999) indicating a seasonal change consistent with general circulation models of Titan. This dataset provides a unique method for determining the amount of light from the surface that penetrates at a given wavelength — a useful metric for constraining radiative transfer models of Titan’s atmosphere.

This research has been supported by an NSF Planetary Astronomy grant to M.E.B. E.L.S. is supported by a Hubble Postdoctoral Fellowship. The data for this program were taken with the Infrared Telescope Facility, which is operated by the University of Hawaii under Cooperative Agreement no. NNX08AE38A with the National Aeronautics and Space Administration, Science Mission Directorate, Planetary Astronomy Program. This program would not have been possible without the nightly support of telescope operators David Griep, Bill Golisch, Paul Sears, and Eric Volquardsen, who took most of the observations as service

observing. We are grateful to Alan Tokunaga for initially believing in the program, to John Rayner and Bobby Bus for their assistance, and to all IRTF observers whose telescope time was interrupted by our program.

REFERENCES

- Ádámkóvics, M., Wong, M. H., Laver, C., & de Pater, I. 2007, *Science*, 318, 962
- Barnes, J. W., Brown, R. H., Soderblom, L., Buratti, B. J., Sotin, C., Rodriguez, S., Le Mouélic, S., Baines, K. H., Clark, R., & Nicholson, P. 2007, *Icarus*, 186, 242
- Bouchez, A. H. & Brown, M. E. 2005, *ApJ*, 618, L53
- Brown, M. E., Bouchez, A. H., & Griffith, C. A. 2002, *Nature*, 420, 795
- Cushing, M. C., Vacca, W. D., & Rayner, J. T. 2004, *PASP*, 116, 362
- Griffith, C. A., Hall, J. L., & Geballe, T. R. 2000, *Science*, 290, 509
- Griffith, C. A., Owen, T., Miller, G. A., & Geballe, T. 1998, *Nature*, 395, 575
- Griffith, C. A., Penteado, P., Baines, K., Drossart, P., Barnes, J., Bellucci, G., Bibring, J., Brown, R., Buratti, B., Capaccioni, F., Cerroni, P., Clark, R., Combes, M., Coradini, A., Cruikshank, D., Formisano, V., Jaumann, R., Langevin, Y., Matson, D., McCord, T., Mennella, V., Nelson, R., Nicholson, P., Sicardy, B., Sotin, C., Soderblom, L. A., & Kursinski, R. 2005, *Science*, 310, 474
- Hartung, M., Herbst, T. M., Dumas, C., & Coustenis, A. 2006, *Journal of Geophysical Research (Planets)*, 111, 7
- Lorenz, R. D., Mitchell, K. L., Kirk, R. L., Hayes, A. G., Aharonson, O., Zebker, H. A., Paillou, P., Radebaugh, J., Lunine, J. I., Janssen, M. A., Wall, S. D., Lopes, R. M., Stiles, B., Ostro, S., Mitri, G., & Stofan, E. R. 2008, *Geophys. Res. Lett.*, 35, 2206
- Lunine, J. I., Mitri, G., Elachi, C., Stofan, E. R., Lorenz, R. D., Kirk, R. L., Michell, K., Lopes, R. M. C., Wood, C. A., Radebaugh, J., Wall, S. D., Soderblom, L. A., Pallou, P., Farr, T., Stiles, B., Callahan, P., & Cassini Radar Team. 2008, in *Lunar and Planetary Inst. Technical Report, Vol. 39, Lunar and Planetary Institute Conference Abstracts*, 1637–+
- McCord, T. B., Hayne, P., Combe, J.-P., Hansen, G. B., Barnes, J. W., Rodriguez, S., Le Mouélic, S., Baines, E. K. H., Buratti, B. J., Sotin, C., Nicholson, P., Jaumann, R., Nelson, R., & The Cassini Vims Team. 2008, *Icarus*, 194, 212
- McKay, C. P., Pollack, J. B., & Courtin, R. 1989, *Icarus*, 80, 23
- Mitchell, J. T., Pierrehumbert, R. T., Frierson, D. M., & Caballero, R. *PNAS*, 103, 18421.

- Quirico, E. & Schmitt, B. 1997, *Icarus*, 127, 354
- Rannou, P., Montmessin, F., Hourdin, F., & Lebonnois, S. 2006, *Science*, 311, 201
- Rayner, J. T., Toomey, D. W., Onaka, P. M., Denault, A. J., Stahlberger, W. E., Vacca, W. D., Cushing, M. C., & Wang, S. 2003, *PASP*, 115, 362
- Roe, H. G., Bouchez, A. H., Trujillo, C. A., Schaller, E. L., & Brown, M. E. 2005a, *ApJ*, 618, L49
- Roe, H. G., Brown, M. E., Schaller, E. L., Bouchez, A. H., & Trujillo, C. A. 2005b, *Science*, 310, 477
- Roe, H. G., de Pater, I., Macintosh, B. A., & McKay, C. P. 2002, *ApJ*, 581, 1399
- Schaller, E. L., Brown, M. E., Roe, H. G., & Bouchez, A. H. 2006a, *Icarus*, 182, 224
- Schaller, E. L., Brown, M. E., Roe, H. G., Bouchez, A. H., & Trujillo, C. A. 2006b, *Icarus*, 184, 517
- Soderblom, L. A., Tomasko, M. G., Archinal, B. A., Becker, T. L., Bushroee, M. W., Cook, D. A., Doose, L. R., Galuszka, D. M., Hare, T. M., Howington-Kraus, E., Karkoschka, E., Kirk, R. L., Lunine, J. I., McFarlane, E. A., Redding, B. L., Rizk, B., Rosiek, M. R., See, C., & Smith, P. H. 2007, *Planet. Space Sci.*, 55, 2015
- Stofan, E. R., Elachi, C., Lunine, J. I., Lorenz, R. D., Stiles, B., Mitchell, K. L., Ostro, S., Soderblom, L., Wood, C., Zebker, H., Wall, S., Janssen, M., Kirk, R., Lopes, R., Paganelli, F., Radebaugh, J., Wye, L., Anderson, Y., Allison, M., Boehmer, R., Callahan, P., Encrenaz, P., Flamini, E., Francescetti, G., Gim, Y., Hamilton, G., Hensley, S., Johnson, W. T. K., Kelleher, K., Muhleman, D., Paillou, P., Picardi, G., Posa, F., Roth, L., Seu, R., Shaffer, S., Vetrilla, S., & West, R. 2007, *Nature*, 445, 61
- Svensmark, H. & Friis-Christensen, E. 1997, *Journal of Atmospheric and Terrestrial Physics*, 59, 1225
- Thornes, J. E. 2002, *International Journal of Climatology*, 22, 1285
- Tokano, T. 2005, *Icarus*, 173, 222
- Toon, O. B., McKay, C. P., Ackerman, T. P., & Santhanam, K. 1989, *J. Geophys. Res.*, 94, 16287

Table 1. IRTF Titan Observations

UT Date and Time	Ra and Dec	Airmass	Subsolar Long.	Clouds ^a
2006-02-23 07:31:08	08:33:00.78 19:30:56.8	1.040	282.69	
2006-02-24 07:27:13	08:32:47.37 19:31:43.8	1.040	305.16	
2006-03-21 06:28:04	08:28:11.55 19:51:55.0	1.005	147.65	
2006-04-08 05:12:15	08:27:09.89 19:55:07.5	1.008	192.16	
2006-04-09 04:58:36	08:27:06.37 19:54:58.9	1.005	214.54	
2006-04-10 04:53:17	08:27:05.61 19:54:18.0	1.013	237.02	
2006-04-11 05:04:47	08:27:06.48 19:53:45.1	1.005	259.73	
2006-04-17 05:55:42	08:27:54.96 19:52:03.2	1.020	35.680	
2006-04-18 05:54:35	08:28:02.10 19:52:22.3	1.023	58.190	
2006-04-19 05:57:44	08:28:09.00 19:52:29.4	1.030	80.770	
2006-04-30 06:03:35	08:29:25.60 19:45:21.0	1.104	328.87	
2006-05-01 04:50:52	08:29:39.38 19:45:08.4	1.012	350.24	
2006-05-02 05:42:24	08:29:56.81 19:44:38.7	1.078	13.580	
2006-05-14 05:10:39	08:32:27.71 19:34:50.0	1.103	283.61	
2006-05-15 05:08:22	08:32:46.93 19:33:51.6	1.106	306.11	
2006-05-16 05:14:21	08:33:08.39 19:32:45.8	1.127	328.72	
2006-05-17 05:01:22	08:33:29.67 19:31:52.5	1.108	351.04	
2006-05-18 05:04:23	08:33:51.79 19:31:00.4	1.122	13.610	
2006-05-20 05:05:41	08:34:34.46 19:29:32.5	1.143	58.670	
2006-05-28 05:05:41	08:36:47.09 19:20:14.8	1.231	239.08	
2006-05-29 05:15:45	08:37:07.50 19:18:34.2	1.285	261.78	
2006-10-03 14:49:44	09:36:42.31 15:11:24.7	2.082	253.53	
2006-10-05 15:36:37	09:37:30.88 15:07:21.4	1.514	299.35	
2006-10-08 15:15:17	09:38:49.62 15:02:17.0	1.597	6.6000	
2006-10-09 15:46:20	09:39:16.48 15:00:43.0	1.369	29.610	
2006-10-14 15:40:25	09:41:02.50 14:53:55.4	1.307	142.23	
2006-10-22 15:21:24	09:43:21.20 14:41:05.8	1.268	322.34	
2006-10-24 15:39:24	09:44:06.25 14:38:33.9	1.180	7.6700	
2006-10-25 15:30:46	09:44:27.98 14:37:28.6	1.196	30.060	
2006-10-26 15:53:49	09:44:48.48 14:36:29.1	1.122	52.950	0.38%
2006-10-27 15:40:34	09:45:06.87 14:35:35.5	1.146	75.280	

Table 1—Continued

UT Date and Time	Ra and Dec	Airmass	Subsolar Long.	Clouds ^a
2006-10-29 15:27:16	09:45:37.30 14:33:48.2	1.162	120.17	
2006-11-04 14:48:20	09:46:41.12 14:26:57.2	1.214	254.93	
2006-11-09 15:31:12	09:47:56.90 14:22:01.5	1.066	8.2600	0.16%
2006-11-10 15:32:49	09:48:13.08 14:21:35.6	1.058	30.800	
2006-11-11 15:33:27	09:48:27.72 14:21:02.8	1.052	53.340	
2006-11-12 14:54:37	09:48:41.14 14:21:05.5	1.114	75.270	
2006-11-13 15:29:39	09:48:50.32 14:20:16.9	1.047	98.360	
2006-11-14 15:20:42	09:48:59.22 14:19:56.9	1.054	120.77	
2006-11-18 15:33:22	09:49:16.74 14:17:39.9	1.023	211.23	
2006-11-19 15:33:11	09:49:20.48 14:16:58.2	1.020	233.79	
2006-11-20 15:47:51	09:49:25.42 14:16:12.9	1.010	256.56	
2006-11-21 15:35:43	09:49:31.11 14:15:40.3	1.014	278.92	
2006-11-22 15:33:36	09:49:38.44 14:15:01.0	1.013	301.42	
2006-11-23 15:32:57	09:49:48.35 14:14:44.1	1.011	323.93	0.30%
2006-11-24 15:37:15	09:49:57.26 14:15:49.4	1.008	346.54	
2006-11-26 15:26:31	09:50:17.84 14:14:18.2	1.009	31.420	
2006-11-27 15:34:08	09:50:25.47 14:14:29.1	1.006	54.070	
2006-12-05 15:24:42	09:50:22.93 14:14:58.7	1.006	234.36	
2006-12-06 15:30:52	09:50:20.90 14:14:53.5	1.009	257.01	
2006-12-07 15:22:59	09:50:21.18 14:14:52.3	1.008	279.42	
2006-12-08 15:32:06	09:50:21.49 14:14:55.5	1.014	302.12	
2006-12-09 15:42:44	09:50:23.55 14:15:19.1	1.023	324.80	
2006-12-14 15:41:38	09:50:33.29 14:18:04.8	1.042	77.430	
2006-12-17 15:37:34	09:50:16.50 14:20:28.8	1.052	145.02	
2006-12-18 15:38:43	09:50:06.43 14:21:02.8	1.060	167.60	
2006-12-19 15:39:36	09:49:55.69 14:21:40.9	1.067	190.18	
2006-12-20 15:44:54	09:49:44.07 14:22:14.2	1.084	212.83	
2006-12-21 15:49:21	09:49:34.06 14:22:40.5	1.100	235.46	
2006-12-22 15:53:04	09:49:25.46 14:23:11.3	1.117	258.08	
2006-12-23 15:42:39	09:49:18.26 14:23:46.9	1.103	280.45	
2006-12-24 15:43:22	09:49:13.14 14:24:21.3	1.113	303.00	

Table 1—Continued

UT Date and Time	Ra and Dec	Airmass	Subsolar Long.	Clouds ^a
2006-12-27 14:39:10	09:49:01.91 14:27:01.9	1.031	9.5800	
2006-12-28 15:15:23	09:48:57.46 14:28:16.9	1.088	32.660	
2006-12-29 15:19:53	09:48:51.72 14:29:35.2	1.105	55.260	
2006-12-30 15:01:36	09:48:44.78 14:30:36.7	1.078	77.510	
2007-01-02 15:27:09	09:48:06.69 14:35:03.7	1.163	145.57	
2007-01-08 14:21:01	09:46:33.80 14:40:59.8	1.072	279.88	
2007-01-13 15:40:34	09:45:44.95 14:47:55.0	1.405	33.760	
2007-01-14 15:39:56	09:45:33.90 14:49:39.1	1.425	56.270	
2007-01-15 15:40:31	09:45:20.87 14:51:25.8	1.453	78.830	
2007-01-16 09:47:11	09:45:10.55 14:52:41.0	1.259	95.840	
2007-01-17 09:47:54	09:44:53.22 14:54:25.6	1.240	118.39	
2007-02-04 10:21:59	09:39:27.78 15:23:46.6	1.017	164.74	
2007-02-05 10:19:54	09:39:03.15 15:25:18.9	1.016	187.27	
2007-02-06 10:12:50	09:38:39.07 15:26:43.4	1.018	209.73	
2007-02-13 10:39:50	09:36:36.53 15:37:17.8	1.005	7.9100	0.26%
2007-02-15 10:11:40	09:36:07.34 15:41:09.3	1.003	52.520	
2007-02-16 10:01:13	09:35:51.35 15:42:37.4	1.004	74.900	
2007-02-18 11:24:07	09:35:09.00 15:47:00.7	1.063	121.29	
2007-02-20 12:10:54	09:34:21.56 15:50:27.6	1.190	167.13	
2007-02-21 09:53:48	09:33:59.87 15:51:33.2	1.003	187.55	0.15%
2007-02-22 10:00:55	09:33:35.87 15:52:58.4	1.005	210.22	0.19%
2007-02-25 09:16:46	09:32:35.20 15:56:40.0	1.005	277.18	0.17%
2007-02-28 07:54:19	09:31:54.53 16:00:37.4	1.070	343.48	
2007-03-02 09:15:37	09:31:29.05 16:03:54.7	1.002	29.800	
2007-03-03 09:19:56	09:31:16.62 16:05:38.5	1.004	52.390	
2007-03-06 11:30:16	09:30:24.20 16:10:47.2	1.254	122.06	
2007-03-07 10:57:29	09:30:04.86 16:12:10.5	1.159	144.10	
2007-03-08 10:58:04	09:29:43.14 16:13:26.2	1.173	166.68	
2007-03-19 08:13:08	09:27:18.15 16:24:50.9	1.003	52.020	0.22%
2007-03-20 04:51:58	09:27:07.44 16:26:04.2	1.391	71.400	
2007-03-21 05:05:54	09:26:55.04 16:27:23.0	1.301	94.160	

Table 1—Continued

UT Date and Time	Ra and Dec	Airmass	Subsolar Long.	Clouds ^a
2007-03-22 04:52:20	09:26:43.59 16:28:23.9	1.346	116.50	
2007-03-28 07:22:47	09:25:13.31 16:32:20.7	1.002	254.19	0.26%
2007-04-02 05:28:2.	09:24:49.09 16:34:49.6	1.090	5.0600	
2007-04-28 06:21:05	09:23:41.10 16:38:30.8	1.035	232.01	
2007-04-29 04:49:43	09:23:43.30 16:37:52.0	1.008	253.12	0.26%
2007-04-30 04:31:28	09:23:47.99 16:37:06.7	1.016	275.38	
2007-05-06 08:46:35	09:24:46.33 16:34:30.5	1.800	54.520	
2007-05-07 04:42:26	09:24:53.35 16:34:23.0	1.002	73.240	
2007-05-09 04:50:37	09:25:06.39 16:33:35.6	1.003	118.45	
2007-06-08 07:19:22	09:31:57.66 15:58:46.8	2.335	77.020	
2007-06-09 05:09:12	09:32:14.67 15:57:38.1	1.220	97.520	
2007-06-18 05:38:44	09:34:56.68 15:41:17.2	1.545	300.94	
2007-06-19 05:35:52	09:35:22.39 15:39:38.4	1.569	323.42	0.22%
2007-06-21 05:05:23	09:36:14.11 15:36:05.2	1.386	7.9100	
2007-06-22 05:07:02	09:36:41.13 15:34:12.4	1.427	30.560	
2007-10-27 15:15:21	10:33:22.72 10:37:44.8	1.490	23.160	
2007-10-28 15:59:22	10:33:46.77 10:36:09.1	1.247	46.380	0.19%
2007-10-29 15:41:05	10:34:08.58 10:34:38.1	1.308	68.640	
2007-10-30 15:38:43	10:34:28.77 10:33:09.6	1.303	91.130	
2007-10-31 15:46:25	10:34:47.07 10:31:38.0	1.256	113.81	
2007-11-06 14:08:12	10:36:10.38 10:22:04.9	1.748	247.65	0.28%
2007-11-08 15:30:53	10:36:44.75 10:19:00.6	1.207	294.02	0.19%
2007-11-09 15:31:42	10:37:03.69 10:17:27.9	1.193	316.57	
2007-11-10 14:50:07	10:37:22.84 10:16:15.5	1.343	338.46	
2007-11-11 14:58:21	10:37:42.66 10:15:02.4	1.289	1.1100	0.32%
2007-11-12 14:53:25	10:38:01.74 10:13:51.7	1.294	23.560	
2007-11-13 14:44:24	10:38:20.77 10:12:45.4	1.319	45.950	
2007-11-20 15:40:51	10:39:41.46 10:05:35.9	1.078	204.71	
2007-11-21 15:44:03	10:39:48.94 10:04:31.6	1.067	227.34	
2007-11-25 15:40:43	10:40:32.76 10:00:42.4	1.052	317.45	
2007-11-28 15:48:21	10:41:14.44 09:58:51.2	1.033	25.160	

Table 1—Continued

UT Date and Time	Ra and Dec	Airmass	Subsolar Long.	Clouds ^a
2007-12-01 15:46:33	10:41:47.66 09:57:34.6	1.026	92.740	0.23%
2007-12-04 14:47:17	10:42:01.24 09:56:17.5	1.080	159.49	
2007-12-20 15:40:04	10:42:54.34 09:55:30.8	1.025	161.07	
2007-12-21 15:38:31	10:42:49.11 09:55:46.7	1.030	183.60	0.18%
2007-12-23 14:44:47	10:42:37.93 09:56:05.0	1.016	227.89	
2007-12-24 13:55:13	10:42:33.34 09:56:21.5	1.045	249.67	
2007-12-27 13:08:24	10:42:29.66 09:57:31.8	1.100	316.45	
2008-01-03 14:53:51	10:42:19.10 10:03:22.3	1.032	115.95	
2008-01-04 15:01:51	10:42:10.58 10:04:22.2	1.044	138.64	
2008-01-05 15:10:59	10:41:59.32 10:05:12.6	1.060	161.34	
2008-01-06 13:46:15	10:41:48.50 10:06:00.3	1.016	182.59	0.31%
2008-01-07 13:47:25	10:41:35.72 10:06:47.7	1.015	205.17	
2008-01-15 12:44:58	10:40:34.81 10:15:20.9	1.027	24.510	

^aCloud coverage of Titan’s disk. 2σ error bars are $\sim 0.15\%$ on most nights (see Fig 6). Cloud activity is only listed if it is above 0.15% with an error bar less than 0.15% .

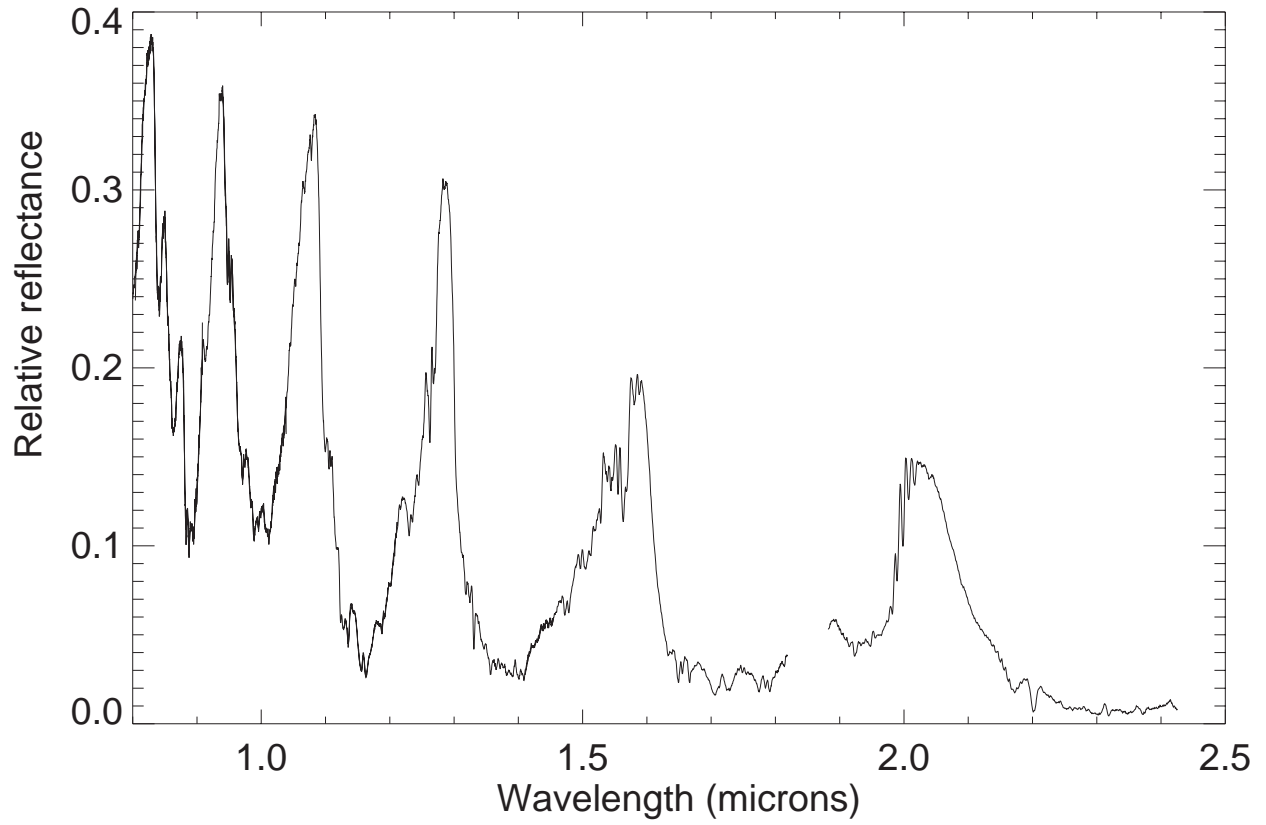


Fig. 1.— Near-Infrared reflectance spectrum of Titan taken with SpeX at the NASA Infrared Telescope Facility on 2008-Jan-04 with a resolution ($R \sim 375$).

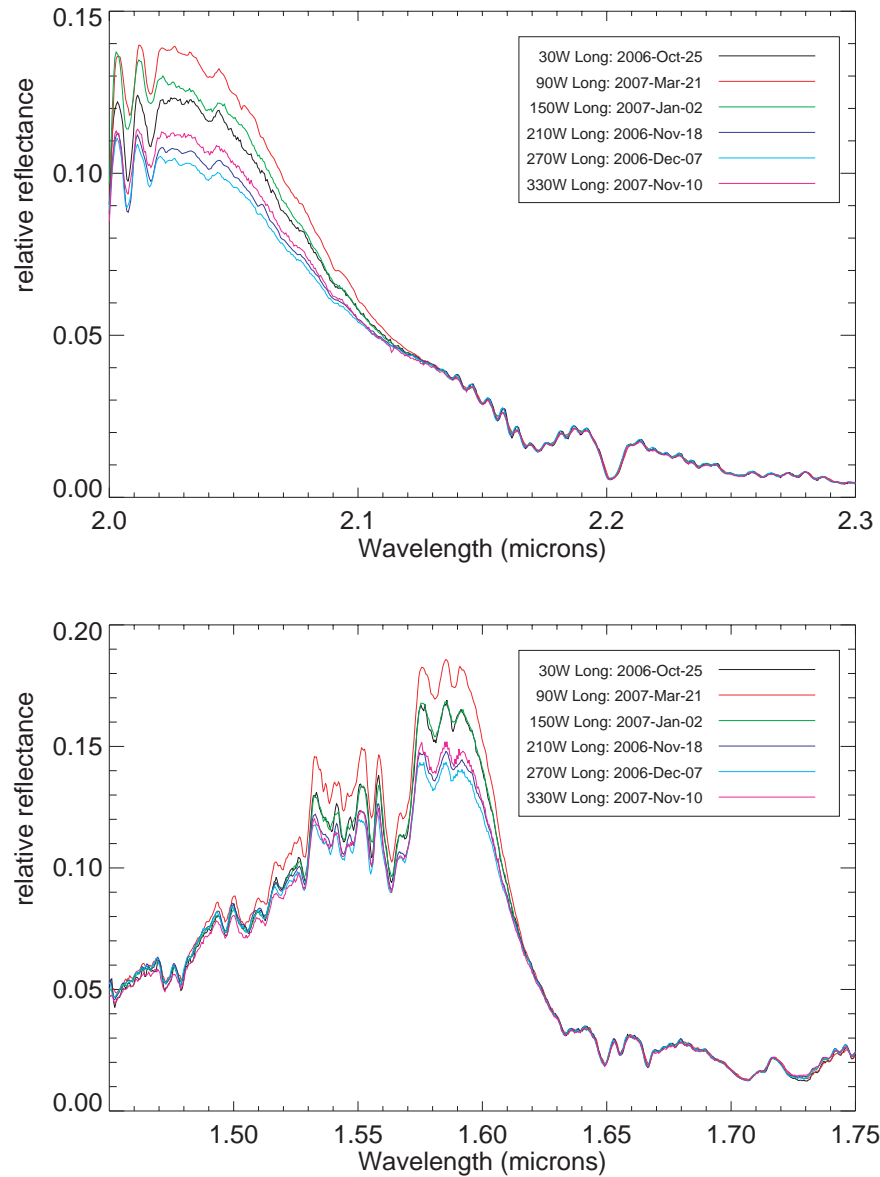


Fig. 2.— Spectra taken at different Titan phases covering the methane window regions in the H and K bands. The spectra lie on top of each other in the high opacity regions (where photons only penetrate to the stratosphere) and differ in low opacity regions (where photons penetrate to the surface and lower atmosphere). The wavelengths at which the spectra deviate from each other, as well as the magnitude of the deviations, allow us to determine if variable tropospheric clouds are present on a given night (see also Figure 5).

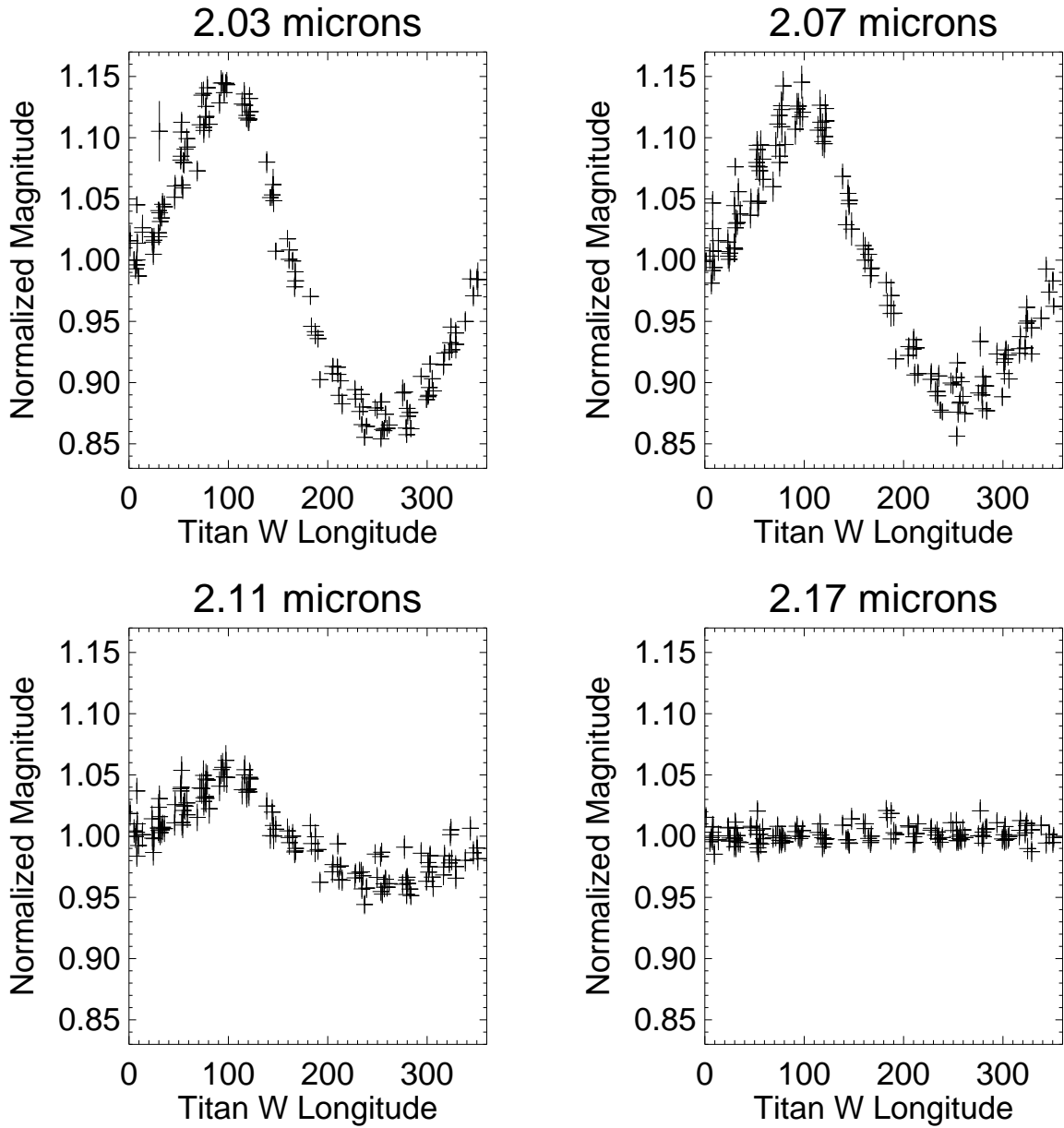


Fig. 3.— K-band lightcurves. The normalized flux at a given wavelength for each of the 138 nights of observations is plotted vs. the Titan central longitude. The magnitude of the lightcurve is greatest near 2.02 microns and decreases with progressively longer wavelengths as Titan’s opacity increases.

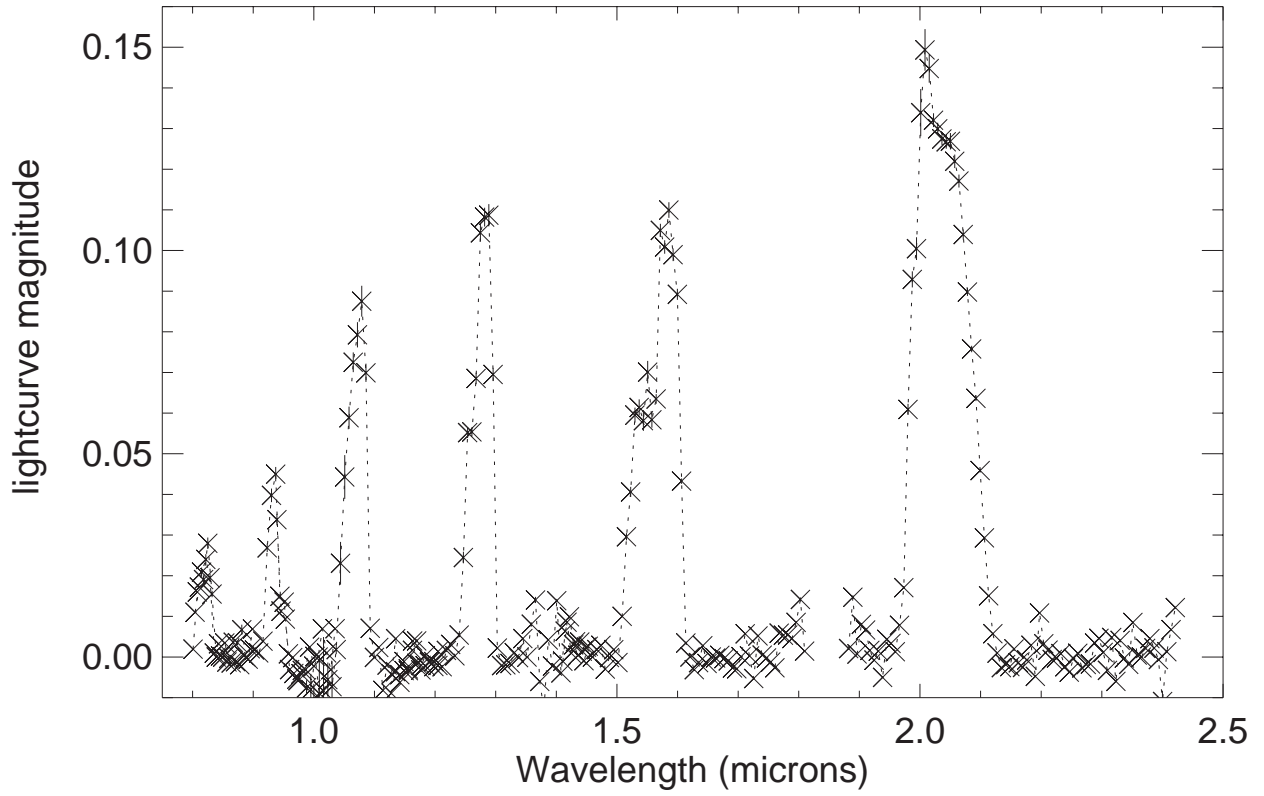


Fig. 4.— Fractional magnitude of Titan’s lightcurve measured in 0.0075 micron wavelength bins. The six surface window regions are clearly visible. Titan’s lightcurve is strongest at 2 microns with a magnitude of $\sim 15\%$.

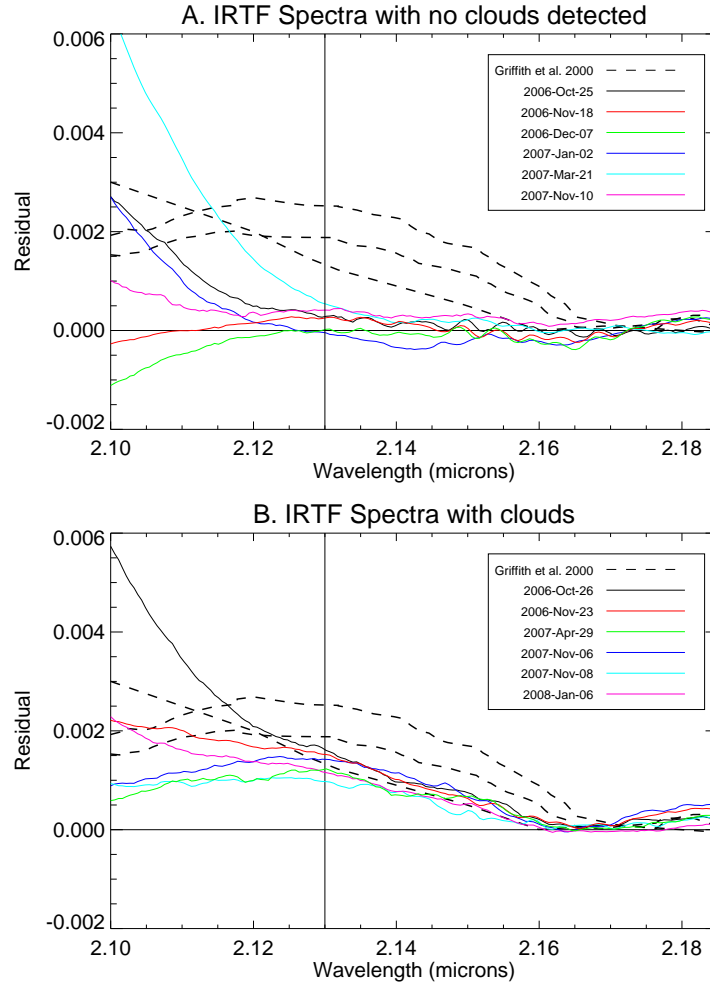


Fig. 5.— A. Titan residual spectra showing no evidence for tropospheric cloud activity. We subtracted a known night of no cloud activity (2006-Feb-23) from all other nights and examine the residual spectra. Longward of 2.17 microns, the spectra all lie on top of each other. The wavelengths at the locations of their deviations tell us about the presence and altitudes of tropospheric clouds. In the absence of clouds, all the spectra will deviate shortward of 2.13 μm (as do 87% of our IRTF spectra). Also shown are typical clouds observed by Griffith et al. (2000) from 1993-1999. These clouds covered 0.3%, 0.5% and 0.7% of Titan’s surface respectively at altitudes of 30 km. B. IRTF spectra with clouds. Similarly to the Griffith et al. (2000) spectra, these spectra deviate at ~ 2.16 microns. However, cloud activity in our observations was much less frequent (only 13% of nights) and generally covered less of Titan’s disk than the Griffith et al. (2000) observations.

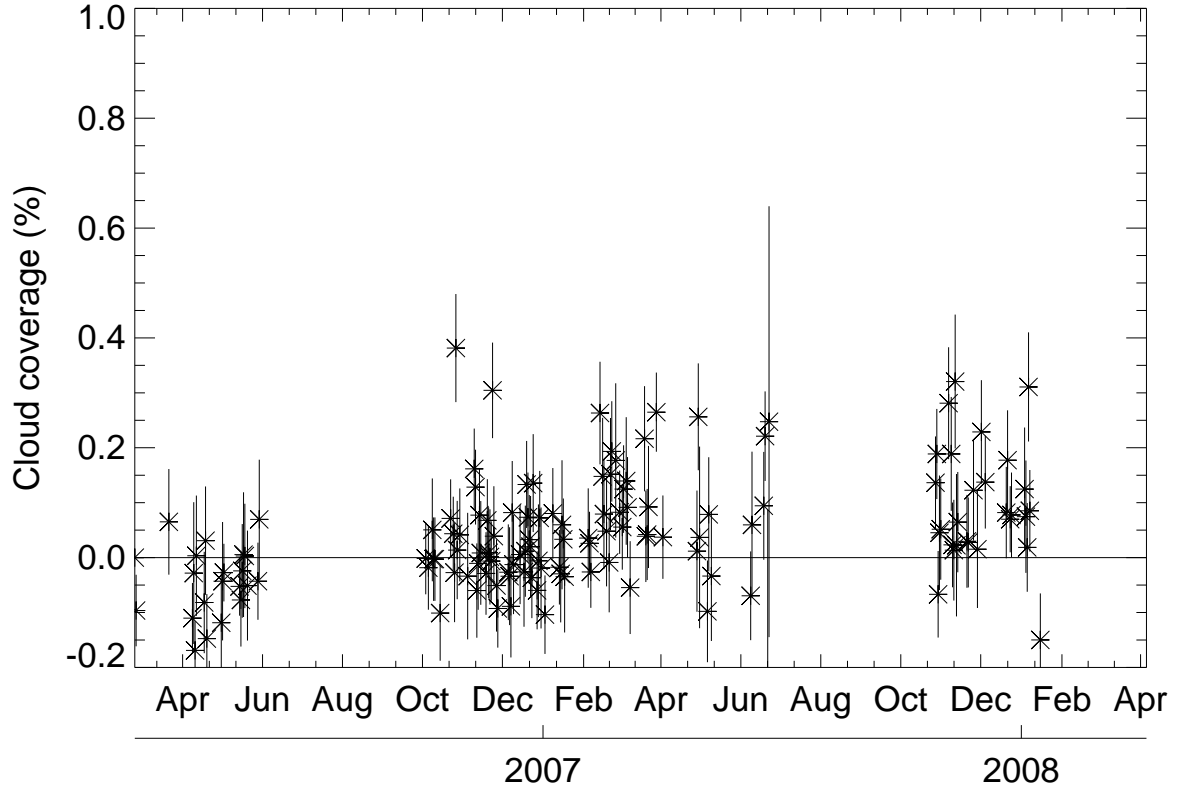


Fig. 6.— Titan residual flux at 2.13 microns allows us to determine the total fraction of Titan’s disk that is covered by clouds (see also Figure 5). We find that on most nights Titan’s clouds covered less than 0.15% of its disk in contrast with the Griffith et al. (2000) observations where cloud activity was detected in nearly all observations covering $\sim 0.5\%$ of Titan’s disk.